



Enhancement of adiabatic effectiveness in a combustion chamber liner with effusion cooling through conical and fan shaped holes

Yellu Kumar^{a*}, Adnan Qayoum^a, Shahid Saleem^a

^aMechanical Engineering Department, National Institute of Technology Srinagar, J&K, 190006, India

*Corresponding author email: yellukumar.rage@gmail.com

Received: 01.11.2023; revised: 15.02.2024; accepted: 20.04.2024

Abstract

The present study involves computational investigation of effusion cooling over a flat plate through the different shaped holes. The interaction between the film jet and the mainstream flow creates a counter-rotating vortex pair, resulting jet detachment from the surface and insufficient film cooling coverage over the surface. To enhance the effusion cooling performance, shaped holes are used in place of standard cylindrical holes to reduce the effects of the counter-rotating vortex pair. Two different shaped holes i.e., conical-shaped and fan-shaped holes are used in the investigation and compared to the cylindrical holes. A commercial finite element method package COMSOL Multiphysics 5.5 is used to simulate and analyse the three-dimensional combustor liners of gas turbine. Data is presented for total 10 rows of effusion holes with injection angles 30° at blowing ratios 0.25, 1.0 and 3.2. The shaped holes provide better cooling effectiveness by increasing the lateral spread of coolant over the surface wall. The results show that both the shaped hole geometries can generate additional anti-counter rotating vortex pairs, which contribute to reducing the strength of the counter-rotating vortex pair. The coolant penetration and strong shear zones at the interaction of coolant jet and main stream in shaped holes are greatly reduced in comparison with cylindrical holes. For a low blowing ratio of 0.25, the conical-shaped holes exhibited adiabatic effectiveness that was 25% and 19% greater than the cylindrical and trapezoidal-shaped holes respectively. On the other hand, fan-shaped holes provide enhanced adiabatic effectiveness at increased blowing ratios. At higher value of blowing ratio 3.2, the adiabatic effectiveness increased by 13% compared to cylindrical holes and 4% compared to conical-shaped holes. In addition, velocity profiles and two-dimensional streamlines have been examined in order to study the flow behavior on the surface.

Keywords: Gas turbine; Combustion chamber liners; Effusion cooling; Adiabatic effectiveness; Conical-shaped holes

Vol. 45(2024), No. 2, 183–193; doi: 10.24425/ather.2024.150864

Cite this manuscript as: Kumar, Y., Qayoum, A., & Saleem, S. (2024). Enhancement of adiabatic effectiveness in a combustion chamber liner with effusion cooling through conical and fan shaped holes. *Archives of Thermodynamics*, 45(2), 183–193.

1. Introduction

Nowadays, aero engines and gas turbines are designed with inlet temperatures ranging from 1 200°C to 1 500°C maintained over extended operational periods to optimize thermal efficiency, which surpasses the metallurgical capacity of their constituent

metals [1–4]. As a result, a proficient cooling system becomes essential for elongating the operational lifespan of the high-temperature components within a gas turbine engine such as the combustion chamber liners, turbine blades and nozzles. The secondary fluid/coolant fluid is allowed to pass through discrete holes drilled on the surface of hot components involved in form-

Nomenclature

d	– diameter of effusion hole, m
t	– thickness of effusion plate, m
S_x/d	– streamwise distance between two adjacent holes in x -direction
S_y/d	– spanwise distance between two adjacent holes in y -direction
T	– temperature, K
U	– flow velocity, m/s
X	– streamwise coordinate, m
Y	– spanwise coordinate, m
Z	– normal coordinate, m

Greek symbols

α	– injection angle, °
----------	----------------------

ing a thin film layer on the hot surface which acts as a thermal shield between the hot gases and metal components. Film cooling and effusion cooling (full coverage film cooling) are more efficient than other cooling strategies [5]. However, the former cooling method does not provide enough cooling due to the discrete nature of holes. In contrast, in the latter one, many holes are arranged in an array to ensure full coverage protection on the surface. The overall effusion cooling effectiveness is dependent on both geometrical and flow parameters like coolant hole diameter, spacing of holes, coolant injection angle, base material thermal conductivity, density ratio, blowing ratio (BR) and momentum flux ratio, etc. Tests are being carried out using a flat plate designed to resemble an actual combustion chamber liners of gas turbine engine. The purpose of these tests is to enhance our comprehension of the fluid dynamics between the main air-flow and the coolant flow.

Andrews et al. [6–8] conducted experiments to examine the effects of geometrical parameters such as the diameter of injection hole, shape of coolant hole, and injection angle on the effusion cooling performance. Kumar et al. [9, 10] studied the effect of blowing ratio and enhancement of adiabatic effectiveness by placing an upstream ramp in front of the effusion holes. The authors [11, 12] investigated both experimentally and numerically to determine the effects of hole spacing in streamwise and spanwise directions and different coolant injection angles and deflection angles, all while measuring the adiabatic film effectiveness at various BRs. Kumar et al. [13] have compiled a comprehensive review of effusion cooling system performance. The study results demonstrated a statistically significant relationship between various parameters and adiabatic efficiency. The above literature studies indicated that the adiabatic effectiveness gradually increases from starting holes to ending holes by the lateral spreading of coolant by the adjacent holes.

Later, researchers have focused their effects on improving the overall efficiency of cooling performance by conducting numerous experimental and numerical methods on shaped holes. A well-known fact is that expanded exits in hole geometries can greatly enhance cooling performance by allowing coolant to spread laterally over the surface. Expanding the exit of the hole leads to a reduction in the velocity of the coolant as it exits. The decrease in velocity helps to minimize lift-off without penetration, allowing the coolant to spread out over a larger area more effectively, allowing the coolant to spread out over a larger area

η	– adiabatic effectiveness
$\bar{\eta}$	– area-averaged adiabatic effectiveness
ρ	– density, kg/m ³

Subscripts and Superscripts

∞	– mainstream flow
c	– coolant flow
wt	– wall temperature on adiabatic surface of effusion plate

Abbreviations and Acronyms

ACRVP	– anti-counter rotating vortices pair
BR	– blowing ratio
CRVP	– counter rotating vortices pair
DR	– density ratio
VR	– velocity ratio

more effectively. This coolant coverage over the optimizes heat transfer efficiency by ensuring greater contact between the cooling fluid and the heated surface thereby enhancing cooling effectiveness. However, the counter-rotating vortices pair (CVRP) generated by the coolant jet with the interaction of mainstream flow, might degrade the cooling efficiency on the surface by causing aerodynamic lift. Due to their rotational direction, these vortices enable the hot mainstream gases to flow beneath the coolant jet, leading to elevated temperatures on the surface. The anti-contour rotating vortex pairs (ACRVPs) are generated when the coolant jet interacts with the high-speed mainstream flow, leading to the formation of vortices that rotate in opposite directions of CRVPs. The formation ACRVPs in effusion cooling systems significantly enhances cooling effectiveness by providing better mixing, increasing surface coverage, disrupting the thermal boundary layer and enhancing convective heat transfer. It is crucial to elevate the lateral expansion of the coolant jets to optimize the cooling effectiveness at an increased distance downstream from the coolant jet outlets. Therefore, in order to attain enhanced cooling performance on the effusion plate, it becomes crucial to alter the flow patterns. Some of the possible ways to alter the flow structures are: 1) to altering the boundary-layer/cooling jet interactions, 2) by modifying the flow upstream of the coolant jet, 3) modifying the shape of hole geometry. Goldstein et al. [14] were the first to introduce the concept of shaped cooling holes to enhance the film cooling process. A comparison was done between the inclined cylindrical holes and 12° laterally expanded exit holes. According to the effectiveness data, the results show that the shaped film holes provide better film cooling protection.

Zing and Zhang [15] conducted numerical simulations to examine the depth of a contoured hole known as a crater, affecting both the downstream flow field and the effectiveness of adiabatic cooling across a range of blowing ratios. Prasanna et al. [16] concluded that the 3D hybrid slot-effusion setup offers significant benefits in enhancing film cooling effectiveness and decreasing cooling nonuniformity. Huang et al. [17] investigated a multi-objective optimization process aimed at refining the shape of the round to slot holes (RTSH). In the process two independent objective functions the discharge coefficient (C_d) and spatially-averaged adiabatic film cooling effectiveness were utilized. Hao et al. [18] examined film cooling performance both experimentally and numerically, revealing that larger compound

angles exacerbate the effects under lateral pressure gradients, in stark contrast to findings observed in zero pressure gradient environments. Park et al. [19] conducted experimental investigations on the film cooling effectiveness concerning three parameters of a fan-shaped hole: the forward expansion angle, lateral expansion angle, and metering length ratio. Their findings indicated that increasing the forward and lateral expansion angles, along with reducing the metering length ratio, led to an overall enhancement in film cooling effectiveness. Li et al. [20] investigated the adiabatic effectiveness of three different arrangements of tangential inlet cooling holes and their respective cooling efficiencies. They observed that the cooling film produced by the tangential jet adopts a divergent "horsetail" shape, closely adhering to the inner wall of the liner. The tight adherence of horsetail increases both the cooling area and effectiveness. The authors [21–23] demonstrated that compound-angle injection has cooling effectiveness over simple-angle injection. The coolant jet ejected from the compound-injection holes provides more lateral spread over the surface than the normal cylindrical holes as the coolant travels downward. Thole et al. [24] demonstrated the turbulence and velocity flow field measurements of cylindrical, forwarded diffused fan-shaped, and laterally diffused fan-shaped holes. The results show that the laterally diffused holes provide better cooling performance by producing less coolant jet penetration, reducing the velocity and turbulence gradients than the round holes. Bell et al [25] measured the adiabatic effectiveness of film cooling and other performance parameters for different shaped holes: (i) cylindrical simple angle holes, (ii) laterally diffused coolant holes, (iii) laterally diffused compound angle holes, (iv) forward diffused simple angle holes, and (v) forward diffused compound angle (FDCA) holes. Their findings demonstrated that the cooling protection provided by laterally diffused compound angle (LDCA) holes is more effective compared to other hole geometries for a wide range of Blowing ratios. Schmidt et al. [26] studied the combined effects of compound angle with expanded exit on the flat plate. They concluded that forward expanded holes with compound angles 60° provide better film cooling than other configurations. From the past literature studies, Researchers have made efforts to improve the overall effusion cooling performance by modifying the flow and geometrical parametric conditions. However, the shaped holes with expanded exits enhanced the film cooling performance.

The objective of this paper is to quantify the downstream adiabatic effectiveness in the streamwise direction of effusion holes. The primary focus of this study is on two types of hole geometries: fan-shaped and a novel conical-shaped hole. The local adiabatic effectiveness and area-averaged adiabatic effectiveness are measured for both the fan-shaped and conical-shaped holes and subsequently compared to the baseline model represented by cylindrical holes. The investigations are carried on 10 rows of effusion holes with injection angle 30° at BRs 0.25, 1.0 and 3.2. The BRs taken are low BR 0.25, intermediate BR 1.0, and high BR 3.2. The velocity profiles and two-dimensional stream lines are investigated just downstream of the first and last row of effusion holes for obtaining a complete physics

of the flow behavior over the flat plate under the influence of effusion cooling.

2. Numerical methods

2.1. Geometry

Figures 1 and 2 shows the schematic of computational model and details of effusion plate for cylindrical holes (baseline). The computational domains consist of three segments i.e., mainstream flow, effusion plate and coolant flow. Hot gases are directed to pass over the effusion plate within the mainstream duct, while coolant air is introduced through the effusion holes into the same mainstream duct. The effusion plate consists of 10 rows of holes arranged in a staggered pattern. The diameter of coolant injection holes (d) is 5.7 mm. The spacing of holes in streamwise and spanwise direction $S_x/d = 4.6$ and $S_y/d = 2.4$. The thickness of the effusion plate (t) is 3d and the coolant is injected into the mainstream flow at (α) is 30°. The dimensions of mainstream duct are 130d (x-direction) and 10d (y-direction). The symmetric boundary conditions are applied on either side of the computational domain in the y-direction.

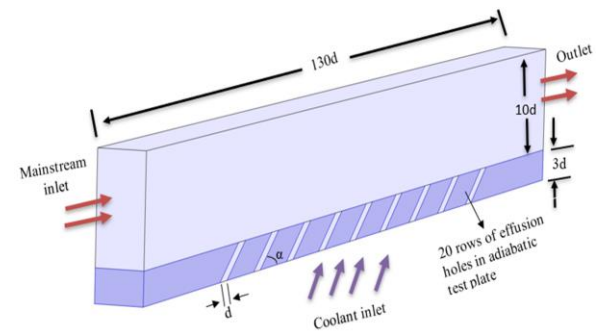


Fig. 1. Isometric view of computational domain and boundary conditions.

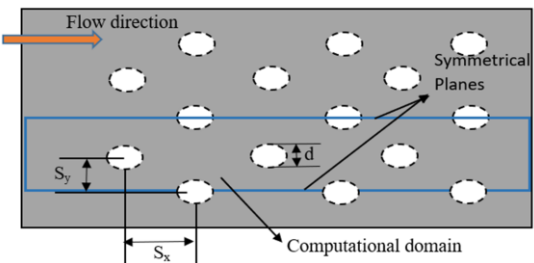


Fig. 2. Top view of computational domain on effusion plate surface (XY plane).

Three different hole geometries (cylindrical, conical, and fan-shaped holes) are used as cooling injection holes as shown in Fig. 3. The conical-shaped holes have an expanded exit of 10° in both x-direction and y-direction. However, the inlets of the conical shaped holes and fan-shaped holes are equal to diameter d same as of cylindrical holes.

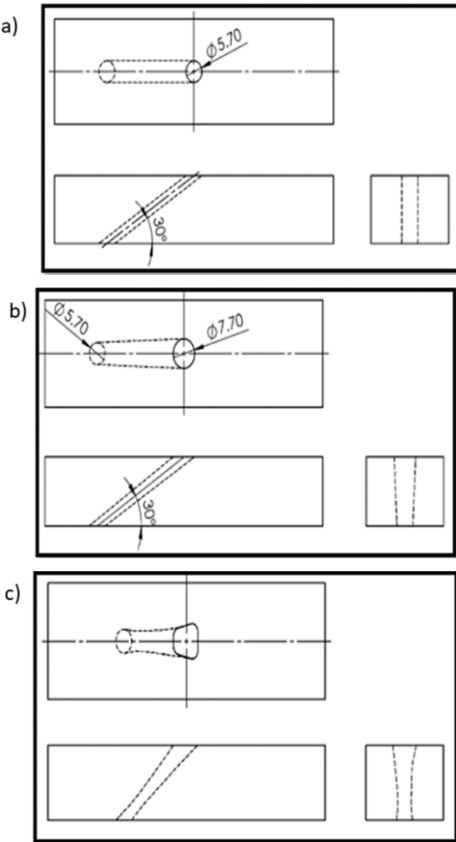


Fig. 3. Sketch map of different hole geometries:
(a) cylindrical holes, (b) conical, (c) fan-shaped hole.

2.2. Boundary conditions

Air is used as a working medium for both mainstream and coolant flow. Both the inlets are set as velocity inlets, and the outlet of mainstream flow is set as a static pressure outlet. The velocity of mainstream flow is constant at $V_\infty = 50$ m/s, and the coolant velocities V_c are varied according to the required BR. The inlet temperatures of mainstream flow and coolant flow are uniformly maintained at 350 K and 300 K respectively. The effusion plate was made of urethane foam with a low thermal conductivity $k = 0.029$ W/(m K) resulting in a maximum conduction loss to allow for adiabatic surface temperature measurements. Consequently, the effusion plate is configured as an adiabatic plate, so conduction and internal cooling in holes are negligible. A complete list of all the combination of the various parameters used in the investigation are tabulated in Table 1.

Table 1. Boundary conditions.

Surface	Boundary conditions
Mainstream inlet	Velocity inlet
Coolant inlet	Velocity inlet
Test plate	Adiabatic wall
Mainstream outlet	Pressure outlet
Sides of mainstream flow	Wall with symmetry
Coolant hole wall	Wall with symmetry

2.3. Measurement and parameter definition

Blowing ratio is the key parameter used to investigate the effect of coolant flow velocity on effusion cooling performance with a constant mainstream flow. The BR is defined as the coolant mass flux to mainstream mass flow:

$$\text{BR} = \frac{\rho_c U_c}{\rho_\infty U_\infty}, \quad (1)$$

where ρ_c and U_c are the density and velocity of coolant flow at effusion hole exit, respectively, and ρ_∞ and U_∞ are the density and velocity of mainstream flow. The BRs used in these studies are 0.25, 1.0, and 3.2.

The effusion cooling performance is measured by the adiabatic effectiveness on the centerline of symmetrical plane and is defined as:

$$\eta = \frac{T_\infty - T_{wt}}{T_\infty - T_c}, \quad (2)$$

where T_{wt} is the adiabatic wall temperature after the exposure of coolant flow on the effusion plate, T_∞ and T_c are the temperatures of mainstream and coolant flow.

The area-averaged adiabatic effectiveness measured in the area between the leading edge of the effusion plate to trailing edge of the plate by considering the local adiabatic effectiveness i.e X_{start} to X in streamwise direction and Y_{start} to Y in spanwise direction:

$$\bar{\eta} = \frac{1}{|x_{start} - x|} \frac{1}{|y_{start} - y|} \int_{x_{start}}^x \int_{y_{start}}^y \eta(x, y) dx dy. \quad (3)$$

2.4. Computational details and validation test

The commercial software COMSOL Multiphysics 5.5 is utilized to solve the three-dimensional steady, incompressible, and turbulent flow. Employing an appropriate turbulence model in simulations becomes crucial to achieve precise forecasts of the flow pattern and temperature distribution across the effusion surface. Previous research studies showed that the $k-\varepsilon$ model could predict the centerline adiabatic effectiveness and velocity flow [27,28]. In order to determine the adiabatic effectiveness on the effusion surface, a number of validation test runs are carried out before starting the computations for the model.

The present simulation results are validated by comparing with the experimental results of Scrittore et al. [29]. The geometrical and flow parameters were strictly followed to validate the simulation results as in ref [29]. The validation test run was carried for cylindrical holes at high BR 3.2 for 20 rows of effusion holes.

The comparison of experimental and computational results for centerline adiabatic efficiency along the streamwise is shown in Fig. 4. The current findings show a good agreement with the experimental data. However, to reduce the computational run time the holes in the effusion region were reduced to 10 rows of holes for all geometrical models. The small variances between the computational and experimental outcomes in the initial rows might stem from the experimental conditions not being entirely adiabatic.

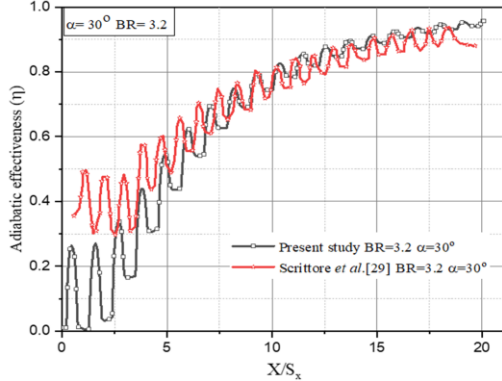


Fig. 4. Comparison of centerline adiabatic effectiveness of computational results with experimental results [29] for BR = 3.2.

2.5. Grid distribution and convergence criteria

A grid independence study was performed to ensure that the results obtained were independent of the mesh size. The grid size has an impact on the accuracy of the results. A user-controlled mesh is applied to the entire domain to obtain the required results. The effusion plate surface is modelled by free triangular mesh with extremely fine grid size, and the remaining domains were modelled with swept mesh. Figure 5 shows the details of computational mesh.

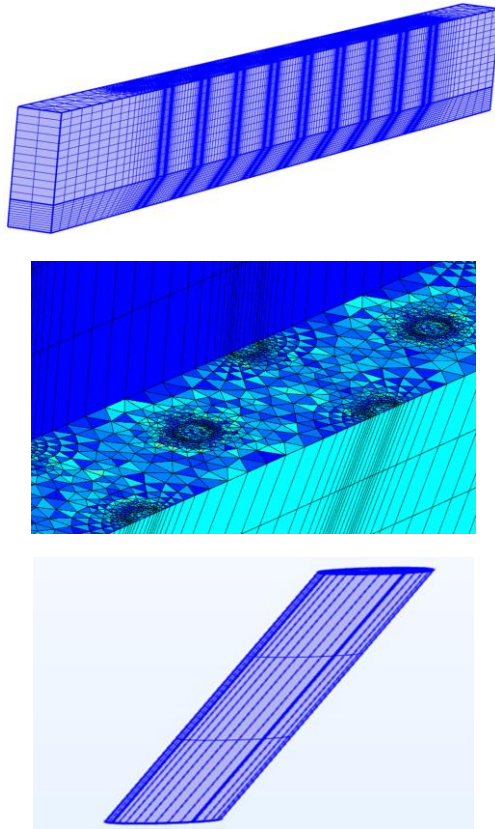


Fig. 5. Computational details: top – entire geometry, middle – effusion plate surface, bottom – effusion hole.

Grid independence study was carried for cylindrical holes with three different grid sizes consisting of 3 631 174, 1 511 096 and 522 762 elements. For proper visualization of temperature counters, better efficiency and computational time economy, a grid size of 1 511 096 elements was chosen for the current simulation. To ensure a mesh of high quality and resolution, the average element quality is maintained at 0.8.

To accurately model the laminar sub-layer and buffer region, the distance of the nearest nodes from the wall is kept at approximately (y^+) = 11.225 for all simulations. To maintain consistency in the modelling approach, a scalable wall function is employed, which adjusts the near-wall mesh to achieve a y^+ value of 11.225. This value corresponds to the beginning of the log-law zone and helps ensure proper representation of near-wall flow dynamics in the simulations. This adjustment is necessary due to the differing levels of resolution in the grid and near-wall refinement caused by variations in geometric and velocity scales within the current model. To prevent the excessive resolution of the laminar sublayer, which is not accurately captured by epsilon-based models, the mesh is internally modified using the scalable methodology.

Convergence criteria has been set such that residuals for the continuity, momenta and turbulent transport equations were required to be below 10^{-5} , while the energy equation residuals had to be below 10^{-8} . Furthermore, the average temperature of the bottom wall is monitored to ensure constant convergence.

3. Results and discussion

The primary focus of this paper was on the computational prediction of adiabatic effectiveness for effusion cooling systems. The effect of the shaped holes and BR on effusion cooling performance is discussed and compared between: (a) cylindrical holes, (b) conical holes, and (c) fan-shaped holes at different BRs 0.25, 1.0 and 3.2 for injection angle $\alpha = 30^\circ$.

3.1. Effect of blowing ratio on adiabatic effectiveness

The centerline adiabatic effectiveness for cylindrical holes at BRs 0.25, 1.0 and 3.2 for injection angle $\alpha = 30^\circ$ is shown in Fig. 6. The figure shows that the BR significantly impacts the adiabatic efficiency of effusion cooling.

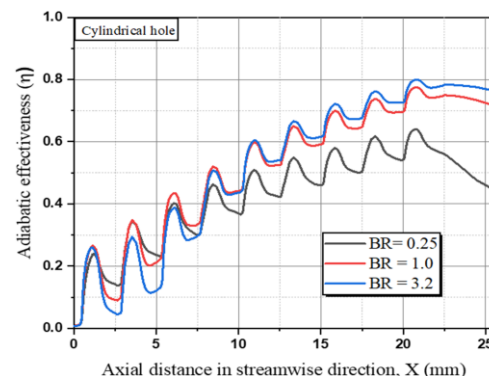


Fig. 6. Comparison of centerline adiabatic effectiveness for cylindrical holes at blowing ratios 0.25, 1.0 and 3.2.

The adiabatic effectiveness peak appears to oscillate increasingly from first row of effusion hole to last row of effusion holes for all blowing ratios. This is due to measurement taken over the effusion plate including coolant holes. The adiabatic effectiveness is high for a low BR until $X/d = 7$. After that, the values decrease compared to high BRs, and opposite behavior is seen for high BRs. The coolant velocity is lower than the mainstream velocity at low BRs and is higher at high BRs. Note that, for low blowing ratios, low coolant mass flow rate is expected from the injection holes and high coolant mass flow rate at high BR. However, the overall performance for each individual shaped hole increases as the blowing ratio increases.

As a result, the coolant jet remains closer to the surface for low BR without penetrating into the mainstream flow and prevents the hot gases from reaching the surface. For this reason, the initial rows just downstream of the coolant holes ($X/d > 5$) are more effective than the latter downstream. Further moving downstream, the adiabatic effectiveness decreases compared to the high BR. Because the hot gases dominate the low coolant mass flow, and the high advection of hot gases causes hot air to be drawn closer to the surface. With decreased coolant fluid mass from effusion holes, it is expected a thin coolant air film will form over the surface as seen in Fig. 7a and Fig. 9, which will be unable to protect the surface from hot gases, leading to a drop in adiabatic efficiency.

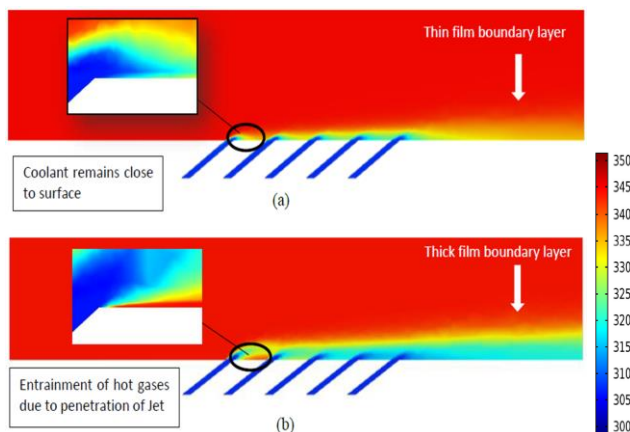


Fig. 7. Penetration of coolant jet in XZ plane for:
a – low blowing ratio 0.25, b – high blowing ratio 3.2.

At higher BRs, the coolant jet penetrates into the mainstream flow for the first few holes, which entrains the hot gases closer to the surface. Downstream in the region (after $(X/d < 5)$), a thick boundary layer of coolant fluid is formed over the surface due to the accumulation of large mass flow rates through effusion holes as seen in from Fig. 7b and Fig. 9. The adiabatic effectiveness is high for high BRs in the downstream region.

3.2. Effect of shaped holes on adiabatic effectiveness

Figure 8 shows the comparison of adiabatic effectiveness at different blowing ratios for conical-shaped and fan-shaped hole. It has been observed that the adiabatic effectiveness of the shaped holes also increases with increased blowing ratios. Because of

the differences in conditions, the level of improvement varies as expected. The trend of adiabatic effectiveness is similarly observed to that of cylindrical holes as discussed in section 3.1.

The rise in adiabatic effectiveness by the shaped holes (varied hole geometries) is attributed to enhancements in all three turbulent mixing process effects associated with the lateral spread of the cooling jets in the vicinity of the cooling holes. The processes are: 1) the mixing process that occurs at the coolant jet's interaction with the main crossflow reduces the strong shear zone, 2) the lateral spread of coolant jet on the surface just downstream of the coolant hole, 3) the mixing process that occurs within the coolant jet itself by weakening the counter-rotating vortices inside the jets as it enters the mainstream.

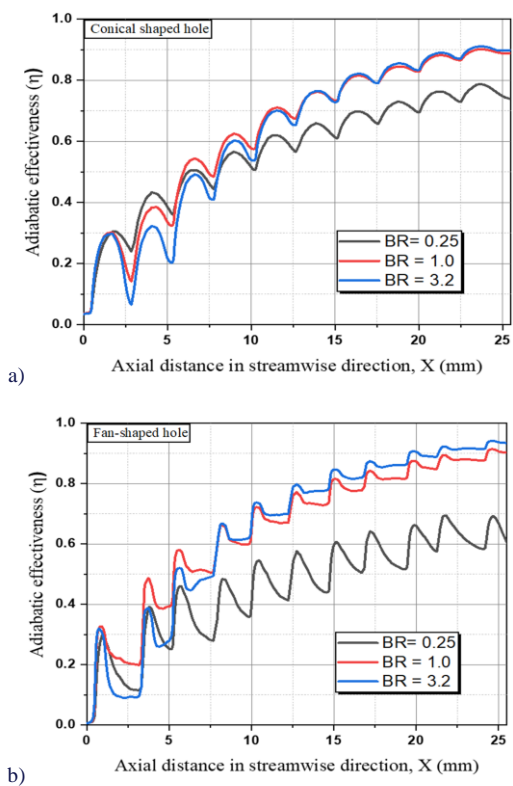


Fig. 8. Comparison of centerline adiabatic effectiveness for blowing ratios 0.25, 1.0 and 3.2: a – conical-shaped holes, b – fan-shaped holes.

Figures 9, 10 and 11 show the temperature contours distribution (cooling effectiveness) on the XY-plane. From Fig. 9, it is observed that for low values of blowing ratios, as the coolant remains close to surface, the temperature contours distribution downstream to the exit of hole geometry in streamwise flow is very thick with coolant jets temperature. But for higher values of blowing ratios, the coolants jet moves away from the surface due to coolants jet lift-off, such that the hot gases reach to the surface. such that the wall temperatures near the holes will be very high. Moving downward in streamwise direction, the wall temperatures are gradually decreased by accumulation of coolant mass flow rate by coalescence of upstream and adjacent effusion holes in turn increases the adiabatic effectiveness.

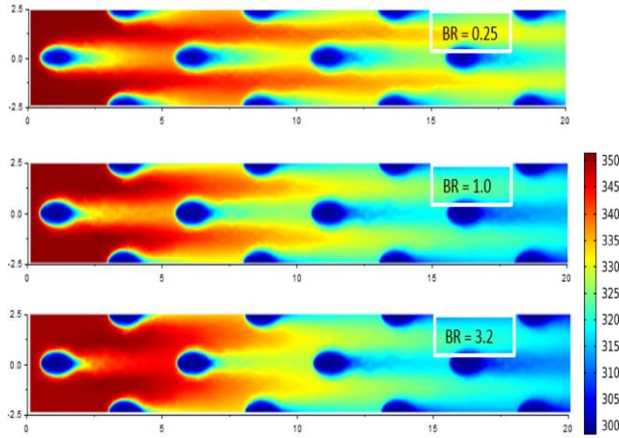


Fig. 9. Surface temperature contours of the effusion plate for cylindrical-shaped hole at different blowing ratios.

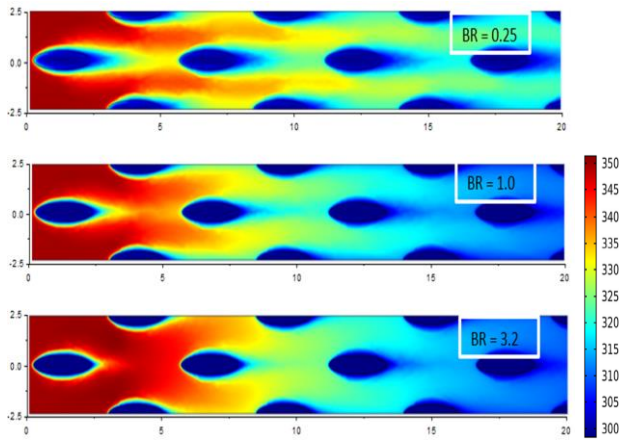


Fig. 10. Surface temperature contours of the effusion plate for conical-shaped hole at different blowing ratios.

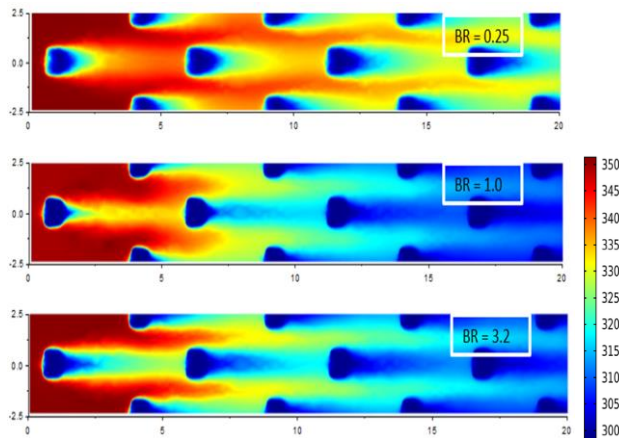
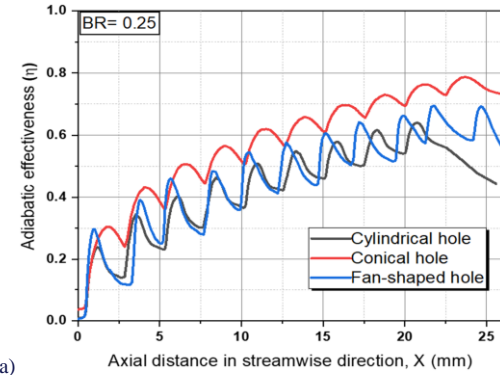


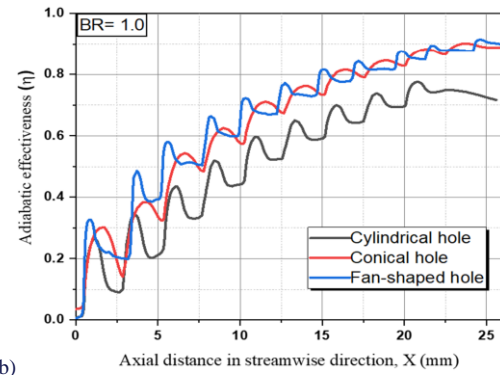
Fig. 11. Surface temperature contours of the effusion plate for fan-shaped hole at different blowing ratios.

From the Fig. 12 for the low values of BR, the conical-shaped holes provide better adiabatic effectiveness than the cylindrical holes and trapezoidal holes. This phenomenon is due to

more lateral spread of coolant downstream of injection holes as the central plane of conical-shaped holes is wider compared to the cylindrical and trapezoidal holes. For such type of holes under steady state flow conditions (low BR) their jets generate anti- counter rotating- vortex pair.



a) Axial distance in streamwise direction, X (mm)



b) Axial distance in streamwise direction, X (mm)

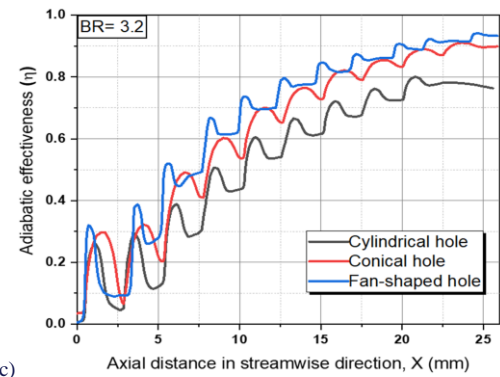


Fig. 12. Comparison of adiabatic effectiveness for different hole geometries at blowing ratios: a) 0.25, b) 1.0 and c) 3.2.

The adiabatic efficiency is increased by the vortex interactions between the jets. For the elevated BR, the fan-shaped holes provide better cooling coverage. When the fan-shaped holes are used, it is expected that mixing at the interface between the coolant jets and the mainstream for a particular coolant flow rate is dramatically reduced near the holes. The decrease in mixing of cross flow and coolant jet is mostly caused by decrease in the jet's velocity as the diffused cross-sectional area at the exit section of fan-shaped holes is more compared to other shaped holes. This slows down coolant jet's lift-off into mainstream flow and remains closer to the surface by enhancing

the adiabatic effectiveness over the surface. In this case, the anti-CRVPs does not exit due to very low velocity caused due to expansion.

3.3. Flow field measurements

The coolant jet flow in conical-shaped hole or the fan-shaped hole expands as it passes through the film cooling hole, which results in the lateral distribution of the jet flow along the spanwise direction. Because of this, the uniformity of coolant jet outflow distribution along spanwise will be greater for the conical hole and fan-shaped hole compared to that of cylindrical hole.

From Fig.13 it is observed that for the cylindrical shaped

holes, the two counter rotating vortices formed is much closer to the centerline of the cut plane by generating more strength to CRVPs, and prevent coolant from spreading over the surface. But the vortices generated in shaped holes moves slightly away from the centerline of cut plane which allows the coolant to spread laterally in spanwise direction. In conical shaped holes, the anti-CRVPs are clearly visible. The temperature boundary layer increases as the coolant flows downstream in the streamwise direction by coalescence of the upstream coolant jet. Furthermore, it is observed the film boundary layer of temperature increases eventually as the coolant flows from row 1 to row 5. The differences in temperature boundary layer for row 1 and row 5 can be seen in the Fig. 13 and Fig. 14.

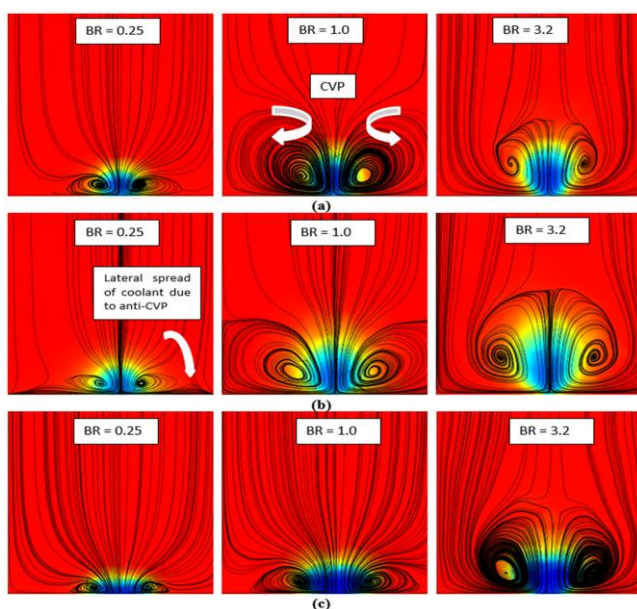


Fig. 13. Streamline-temperature distribution in YZ cut plane downstream of row 1.

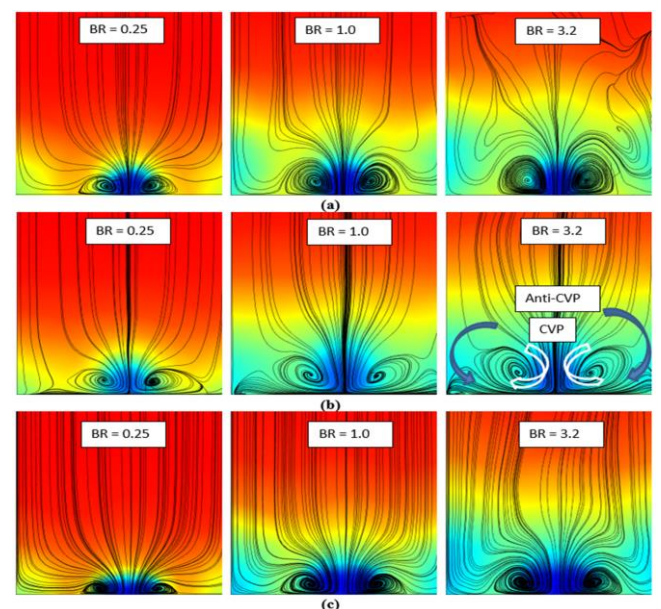


Fig. 14. Streamline-temperature distribution in YZ cut plane downstream of row 5.

3.4. Velocity profile

The velocity profiles are evaluated on the effusion surface downstream of effusion hole at rows 1 and row 5 to determine whether the flow is fully developed or not. The velocity profiles are generated just downstream of corresponding hole in streamwise direction at blowing ratio 0.25, 1.0 and 3.2.

Figure 15 shows the mean velocity profiles for row 1 and

row 5 for blowing ratio 0.25, 1.0 and 3.2, respectively. There is a gradual drop in coolant jet penetration height, as indicated by the maximum streamwise velocity, as the flow moves from row one to row 5. From Fig. 15(b), for cylindrical holes, the maximum peak for row 1 occurs at $0.15d$ and $0.35d$ for row 5. Another interesting phenomenon is that the continuous ejection of coolant flow causes an increase in the velocity of the outer portion of the flow.

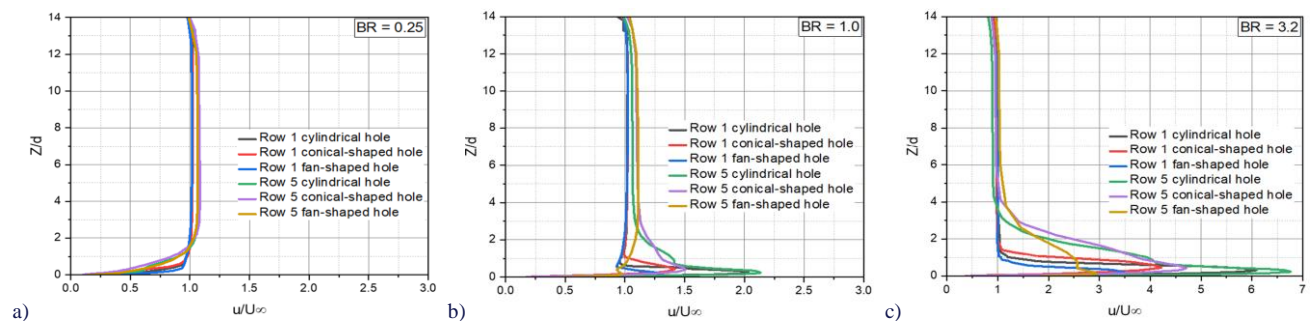


Fig. 15. Stream wise velocity profiles for blowing ratio 0.25, 1.0 and 3.2 just downstream of row 1 and row 5.

As discussed, earlier coolant flow velocity is reduced for shaped holes compared to cylindrical holes. From Fig. 15, the maximum velocity peak in streamwise direction at row 5 for cylindrical holes is $2.2d$, for conical is $1.5d$ and for fan-shaped hole is $0.9d$. These clearly indicates that the velocity of coolant jet has reduced due to expansion of hole exit and there by the lateral spread of coolant increases in both spanwise and streamwise direction as shown in Fig. 16.

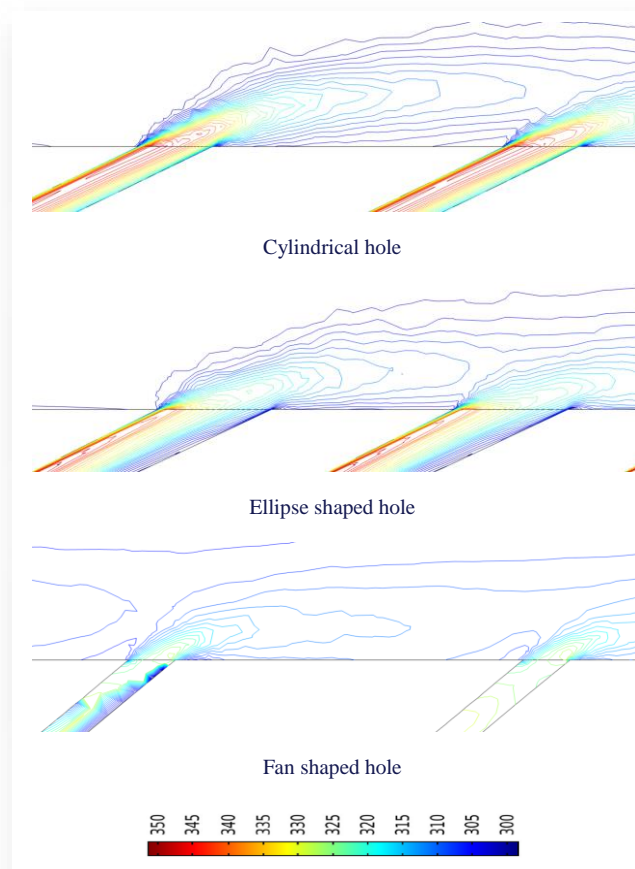


Fig. 16. Velocity distribution and streamlines in the XZ plane cross-section at the exit of holes for BR = 3.2.

Figure 17 illustrates the temperature contour distribution across five cross-sections on the test surface in YZ plane. These cross-sections are positioned downstream of individual injection holes at a distance of $0.5d$ of the effusion holes. It is observed that the trend of the jet cores gradually rises in the streamwise direction. This trend indicates the penetration of coolant from the neighboring holes, resulting in the accumulation of coolant in the downstream direction. When analysing the vortex generator cases in comparison to the Baseline case, it is evident that as the mainstream flow passes through conical and fan-shaped holes, two extra regions of low speed emerge laterally. These regions subsequently interact with the downstream film jet, resulting in a reduction of the jet core's height. This reduction is attributed to the creation of supplementary coherent vortices in a direction opposite to that of the CRVP phenomenon. This trend enhances the lateral expansion of coolant in lateral direction for the shaped holes.

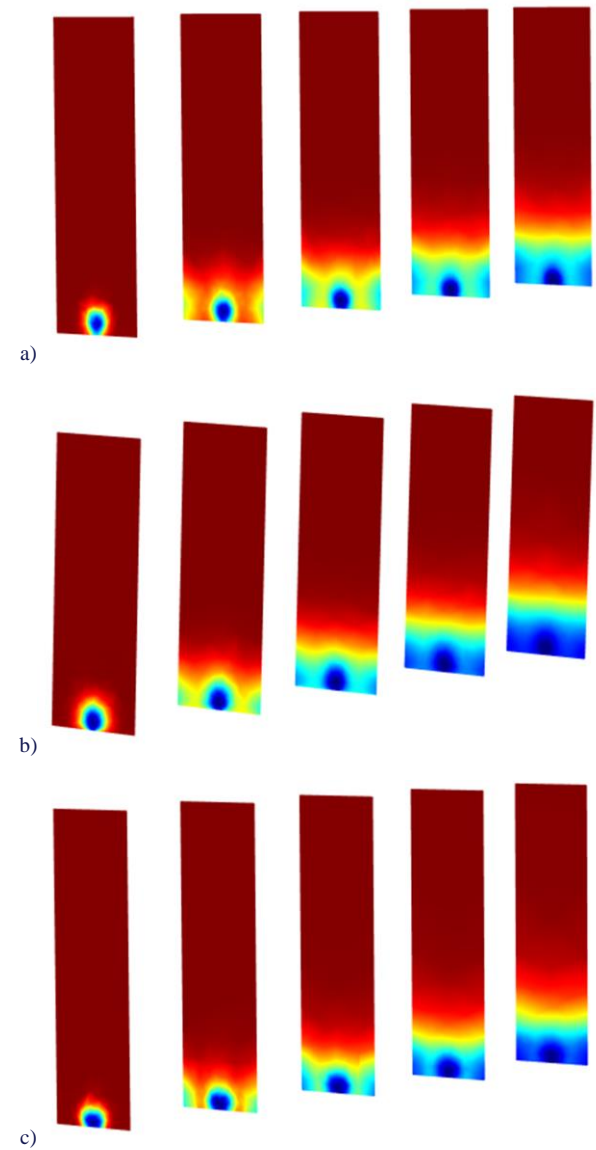
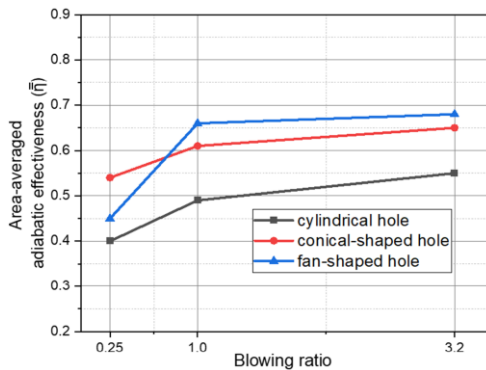


Fig. 17. Temperature contour distribution downstream of film cooling holes in YZ plane for: a) cylindrical holes, b) ellipse shaped holes, c) fan shaped holes.

3.5. Area-averaged adiabatic effectiveness ($\bar{\eta}$)

Figure 18 shows the relation between the blowing ratio and area-averaged adiabatic effectiveness ($\bar{\eta}$). These area-averaged adiabatic effectiveness ($\bar{\eta}$) is represented as overall performance of effusion cooling on the surface. The area-averaged adiabatic effectiveness ($\bar{\eta}$) increases as the blowing ratio increases for all hole geometries. It is clear from Fig. 16 that the conical-shaped and fan-shaped holes provide better cooling effectiveness compared to the cylindrical holes at all blowing ratios. At low BR 0.25, the adiabatic effectiveness of conical-shaped holes was 25% and 19% higher than the cylindrical and trapezoidal shaped holes respectively. For intermediate BR 1.0, the trapezoidal holes provided 21% and 10% higher than cylindrical and conical-shaped holes. Further increasing the blowing ratio to 3.2, the effectiveness increased to 13% and 4% respectively compared to cylindrical and conical shaped hole respectively.

Fig. 18. Area-averaged adiabatic effectiveness ($\bar{\eta}$) vs. BR.

4. Conclusions

The present paper investigates the effect of hole geometries (shaped holes) and coolant jet blowing ratios on effusion cooling performance. The adiabatic effectiveness is measured and compared for three different types of shaped holes (cylindrical hole, conical-shaped hole, and fan-shaped hole) for blowing ratios 0.25, 1.0 and 3.2 at injection angles 30° over a flat surface. In addition, velocity profiles and streamlines on vertical planes are measured at row 1 and row 5 on the flow field.

- Compared to the cylindrical holes, the shaped holes provide more adiabatic effectiveness on effusion plate. The overall adiabatic effectiveness increases as the blowing ratio increases from 0.25 to 3.2.
- At low blowing ratios, the conical-shaped holes are preferable than the cylindrical and fan-shaped holes. The formation of anti-CRVP's at the exit of hole geometry provides more lateral spread of coolant on the surface.
- At high blowing ratios, the fan-shaped holes are preferable than the other shaped holes. Due to diffused shape at the exit of hole's geometry, the coolant jet velocity is reduced which in turn lowers the mixing between the coolant jet and mainstream. This causes the coolant to remain close to the surface and increases the lateral spread of coolant.

At a low blowing ratio of 0.25, conical-shaped holes exhibit 25% and 19% higher adiabatic effectiveness compared to cylindrical and trapezoidal-shaped holes respectively. For intermediate BR 1.0, the trapezoidal holes provided 21% and 10% of adiabatic effectiveness higher than cylindrical and conical-shaped holes. Further increasing the blowing ratio to 3.2, the effectiveness increased to 13% and 4% respectively compared to cylindrical and conical shaped hole respectively.

References

- Yuen, C.H.N., & Martinez-Botas, R.F. (2005). Film cooling characteristics of rows of round holes at various streamwise angles in a crossflow: Part I. Effectiveness. *International Journal of Heat and Mass Transfer*, 48(23–24), 4995–5016. doi: 10.1016/j.ijheatmasstransfer.2005.05.019
- Qayoum, A., & Panigrahi, P. (2019). Experimental investigation of heat transfer enhancement in a two-pass square duct by permeable ribs. *Heat Transfer Engineering*, 40(8), 640–651. doi: 10.1080/01457632.2018.1436649
- Rasool, A., & Qayoum, A. (2018). Numerical analysis of heat transfer and friction factor in two-pass channels with variable rib shapes. *International Journal of Heat and Technology*, 36(1). doi: 10.18280/ijht.360106
- Rasoo, A., & Qayoum, A. (2018). Numerical investigation of fluid flow and heat transfer in a two-pass channel with perforated ribs. *Pertanika Journal of Science and Technology*, 26(4).
- Goldstein, R. J. (1971). Film cooling. In *Advances in Heat Transfer*, 7 (pp. 321–379). Elsevier.
- Andrews, G.E., Alikhanizadeh, M., Tehrani, F.B., Hussain, C.I., & Azari, M.K. (1988). Small diameter film cooling holes: The influence of hole size and pitch. *International Journal of Turbo and Jet Engines*, 5(1–4), 61–72. doi: 10.1515/tjj.1988.5.1-4.61
- Andrews, G.E., Asere, A.A., Gupta, M.L., & Mkpadi, M.C. (1985). Full coverage discrete hole film cooling: The influence of hole size. In *ASME Turbo Expo: Power for Land, Sea, and Air*, 79405, p. V003T09A003 (85-GT-47). doi: 10.1515/TJJ.1985.2.3.213
- Andrews, G.E., Gupta, M.L., & Mkpadi, M.C. (1984). Full coverage discrete hole wall cooling: Cooling effectiveness. In *ASME Turbo Expo: Power for Land, Sea, and Air American Society of Mechanical Engineers*, 79498, V004T09A018 (84-GT-212). doi: 10.1515/TJJ.1985.2.3.199
- Kumar, K.R.Y., Qayoum, A., Saleem, S., & Mir, F.Q. (2022). Effect of blowing ratio on adiabatic effectiveness for effusion cooling in gas turbine combustor liners. *Research on Engineering Structures and Materials*, 8(3), 431–445. doi: 10.17515/resm2022.359me1028
- Kumar, Y., Qayoum, A., Saleem, S., & Mir, F.Q. (2021). Combined effect of upstream ramp and effusion cooling in combustion chamber liners of gas turbines. *Journal of Thermal Engineering*, 9(2), 297–312. doi: 10.18186/thermal.1284759
- Lin, Y., Song, B., Li, B., Liu, G., & Wu, Z. (2003). Investigation of film cooling effectiveness of full-coverage inclined multihole walls with different hole arrangements. In *ASME Turbo Expo: Power for Land, Sea, and Air*, 36886 (651–660). doi: 10.1115/GT2003-38881
- Zhang, C., Lin, Y., Xu, Q., Liu, G., & Song, B. (2009). Cooling effectiveness of effusion walls with deflection hole angles measured by infrared imaging. *Applied Thermal Engineering*, 29(5–6), 966–972. doi: 10.1016/j.applthermaleng.2008.05.011
- Kumar, K.Y., Qayoum, A., Saleem, S., & Qayoum, F. (2020). Effusion cooling in gas turbine combustion chambers – a comprehensive review. In *IOP Conference Series: Materials Science and Engineering*, 804(1), 012003. IOP Publishing. doi: 10.1088/1757-899X/804/1/012003
- Goldstein, R.J., Eckert, E.R.G., & Burggraf, F. (1974). Effects of hole geometry and density on three-dimensional film cooling. *International Journal of Heat and Mass Transfer*, 17(5), 595–607. doi: 10.1016/0017-9310(74)90007-6
- Fu, J.L., Bai, L.C., Zhang, C., & Ju, P.F. (2019). Film cooling performance for cylindrical holes embedded in contoured craters: effect of the crater depth. *Journal of Applied Mechanics and Technical Physics*, 60, 1068–1076. doi: 10.1134/S0021894419060129
- Revulagadda, A.P., Adapa, B.R., Balaji, C., & Pattamatta, A. (2024). Performance assessment and optimization of three-dimensional hybrid slot-effusion jet cooling configuration of an annular combustor liner. *Applied Thermal Engineering*, 240, 122198. doi: 10.1016/j.applthermaleng.2023.122198
- Huang, Y., Zhang, J.Z., & Wang, C.H. (2020). Multi-objective optimization of round-to-slot film cooling holes on a flat surface. *Aerospace Science and Technology*, 100, 105737. doi: 10.1016/j.ast.2020.105737

- [18] Zhang, H., Wang, Q., Chen, Z., Su, X., & Yuan, X. (2020). Effects of compound angle on film cooling effectiveness considering endwall lateral pressure gradient. *Aerospace Science and Technology*, 103, 105923. doi: 10.1016/j.ast.2020.105923
- [19] Park, S.H., Kang, Y.J., Seo, H.J., Kwak, J.S., & Kang, Y.S. (2019). Experimental optimization of a fan-shaped film cooling hole with 30 degrees-injection angle and 6-hole length-to-diameter ratio. *International Journal of Heat and Mass Transfer*, 144, 118652. doi: 10.1016/j.ijheatmasstransfer.2019.118652
- [20] Li, Z., Xie, P., Zeng, Q., & Chen, X. (2023). Study of tangential effusion cooling of a combustor liner. *Processes*, 11(8), 2433. doi: 10.3390/pr11082433
- [21] Schmidt, D.L., Sen, B., & Bogard, D.G. (1996). Film cooling with compound angle holes: adiabatic effectiveness. *Journal of Turbomachinery*, 118(4), 807–813. doi: 10.1115/1.2840938
- [22] Sofi, A.Y., & Qayoum, A. (2023). Numerical investigation of thermo-hydraulic performance and irreversibility behaviour in a pulsating turbulent flow ribbed duct. *Arabian Journal for Science and Engineering*, 49(2), 1515–1529. doi: 10.1007/s13369-023-07902-w
- [23] Qayoum, A., Gupta, V., Panigrahi, P.K., & Muralidhar, K. (2010). Influence of amplitude and frequency modulation on flow created by a synthetic jet actuator. *Sensors and Actuators A: Physical*, 162(1), 36–50. doi: 10.1016/j.sna.2010.05.008
- [24] Thole, K.A., Gritsch, M., Schulz, A., & Wittig, S. (1997). Effect of a crossflow at the entrance to a film-cooling hole. *Journal of Fluids Engineering*, 119(3), 533–540. doi: 10.1115/1.2819277
- [25] Bell, C.M., Hamakawa, H., & Ligrani, P.M. (2000). Film cooling from shaped holes. *Journal of Heat Transfer*, 122(2), 224–232. doi: 10.1115/1.521484
- [26] Sen, B., Schmidt, D.L., & Bogard, D.G. (1996). Film cooling with compound angle holes: heat transfer. *Journal of Turbomachinery*, 118(4), 800–806. doi: 10.1115/1.2840937
- [27] El-Gabry, L.A., & Kaminski, D.A. (2005). Numerical investigation of jet impingement with cross flow – comparison of yang-shih and standard k– ϵ turbulence models. *Numerical Heat Transfer, Part A*, 47(5), 441–469. doi: 10.1080/10407780590891254
- [28] Silletti, M., Divo, E., & Kassab, A.J. (2004). Numerical investigation of adiabatic and conjugate film cooling effectiveness on a single cylindrical film-cooling hole. In *ASME International Mechanical Engineering Congress and Exposition*, 4711, 333–343.
- [29] Scrittore, J.J., Thole, K.A., & Burd, S.W. (2007). Investigation of velocity profiles for effusion cooling of a combustor liner. *Journal of Turbomachinery*, 129(3), 518–526. doi: 10.1115/1.2720492